Geophysical Research Letters

RESEARCH LETTER
10.1029/2024GL110097

The Coldest and Densest Overflow Branch Into the North Atlantic is Stable in Transport, But Warming

Karin Margretha Húsgarð Larsen[1], Bogi Hansen[1], Hjálmar Hátún[1], Guðrið Eriksdóttir Johansen[1], Svein Østerhus[2], and Steffen Malskær Olsen[3]

[1]Faroe Marine Research Institute, Tórshavn, Faroe Islands, [2]NORCE Norwegian Research Centre and Bjerknes Centre for Climate Research, Bergen, Norway, [3]Danish Meteorological Institute, Copenhagen, Denmark

Key Points:

- Observed Faroe Bank Channel overflow strength has been stable from 1996 to 2022, but the overflow waters warmed in the recent two decades
- Concurrent salinity increase prevented the bottom water density from decreasing significantly from the effect of warming
- After entrainment downstream, the overflow contributed water of reduced density to global overturning due to non-linear effects of warming

Supporting Information:

Supporting Information may be found in the online version of this article.

Correspondence to:

K. M. H. Larsen,
KarinL@hav.fo

Citation:

Larsen, K. M. H., Hansen, B., Hátún, H., Johansen, G. E., Østerhus, S., & Olsen, S. M. (2024). The Coldest and densest overflow branch into the North Atlantic is stable in transport, but warming. *Geophysical Research Letters*, *51*, e2024GL110097. https://doi.org/10.1029/2024GL110097

Received 6 MAY 2024
Accepted 8 AUG 2024

Abstract

The overflow of cold water through the Faroe Bank Channel (FBC) is the densest water crossing the Greenland-Scotland Ridge and the densest source for the Atlantic Meridional Overturning Circulation (AMOC). Here, we show that the overflow volume transport remained stable from 1996 to 2022, but that the bottom water warmed at an average rate of 0.1°C per decade, mainly caused by warming of deep waters upstream. The salinity of the overflow water has increased as a lagged and reduced response to the salinity increase seen in the upper-layer source waters. Therefore, the potential density of the bottom water over the FBC sill shows no statistically significant trend. After entrainment of warmer ambient waters downstream of the FBC, the nonlinear density dependence upon temperature implies, however, that the overflow contributed water of reduced density to the local overturning and the deep limb of the AMOC.

Plain Language Summary

As part of the Atlantic Meridional Overturning Circulation—often called AMOC—dense water is formed north of the subsea ridge between Greenland and Scotland. On its route southward at depth, the dense water has to cross this subsea ridge called the Greenland-Scotland Ridge. The densest water flows through the deepest trench, which is the Faroe Bank Channel with a sill depth of 840 m. Here, the strength of the flow has been monitored since 1995 together with its temperature and salinity characteristics. While the strength of the flow has been stable throughout the monitoring period, the dense water in the Faroe Bank Channel has warmed and also become more saline. Despite the warming, the density of the water, which is determined by the combination of temperature and salinity, has remained nearly unchanged. After leaving the Faroe Bank Channel, the dense water intensively entrains and mixes with warmer surrounding water and forms a larger volume of water, termed Iceland-Scotland Overflow Water, that feeds the AMOC. The density of this large volume is sensitive to warming. The observed warming of the dense water may, therefore, have implications for the AMOC and thereby on the regional as well as global climate.

1. Introduction

With a sill depth of 840 m (Figure 1), the Faroe Bank Channel (FBC) is the deepest passage across the Greenland-Scotland Ridge, and through this channel, there is a continuous flow of cold water, termed FBC-overflow (Borenäs & Lundberg, 1988; Hansen & Østerhus, 2007; Hermann, 1959). Using the traditional criterion, $\sigma_\theta > 27.8$ kg m^{-3}, to define overflow water (e.g., Dickson & Brown, 1994), Hansen and Østerhus (2007) estimated the average volume transport of FBC-overflow in the 1995–2005 period to be (1.9 ± 0.3) Sv (1 Sv = 10^6 m^3 s^{-1}). By this criterion, the FBC-overflow transports around one third of the total overflow across the ridge (Østerhus et al., 2019), making it second in strength after the Denmark Strait overflow. The densest component of the FBC-overflow is colder and denser than the densest component of the Denmark Strait overflow (Huang et al., 2020) and the other, weaker, overflow branches (Beaird et al., 2013; Johnson et al., 2017; Østerhus et al., 2008).

The FBC-overflow, thus, is the coldest and densest source for the deep limb of the Atlantic Meridional Overturning Circulation (AMOC). It is, however, strongly modified by entraining ambient water masses on route toward the deep Atlantic Ocean. Much of the water mass transformation occurs within a short distance from the FBC exit (Geyer et al., 2006; Mauritzen et al., 2005; Ullgren et al., 2016). Together with the weaker Iceland-Faroe Ridge (IFR) overflow (Beaird et al., 2013), the FBC-overflow leaves the Iceland Basin as Iceland-Scotland Overflow Water (ISOW). ISOW is composed of the overflow water masses Norwegian Sea Overflow Water (NSOW) and Modified East Iceland Water (MEIW) and the ambient water masses Labrador Sea Water (LSW) and Subpolar Mode Water (SPMW). The FBC-overflow carries NSOW, while the IFR-overflow carries both NSOW and MEIW. However, details of IFR-overflow are still missing (Johns et al., 2021). Observations indicate

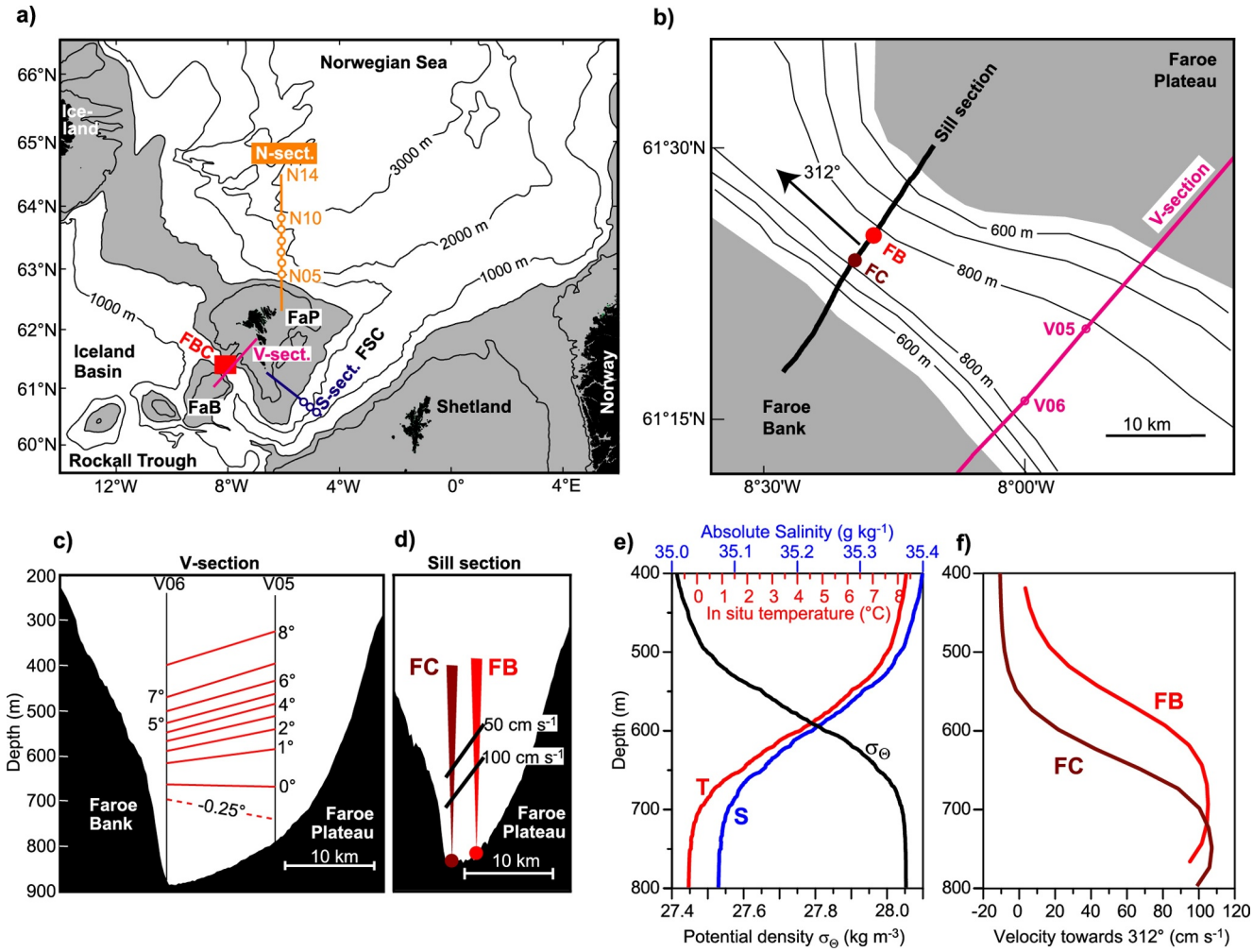

Figure 1. Monitoring setup and average conditions for the FBC-overflow in the 1996–2022 period. (a) Map of the region with bathymetry based on GEBCO. Areas shallower than 500 m are gray. "FBC" is Faroe Bank Channel. "FaB" is Faroe Bank. "FaP" is Faroe Plateau. "FSC" is Faroe-Shetland Channel. The red rectangle in the FBC shows the area covered by the expanded map in (b). Three CTD standard sections are indicated by differently colored lines with selected standard stations indicated by circles in the same colors. (b) Expanded map of the FBC sill region (red rectangle in (a)) showing bottom topography, the two ADCP deployment sites (FB and FC), and two standard CTD stations (V05 and V06) on the V-section. (c) The V-section showing average isotherms below 200m depth is based on 104 CTD profiles at each station in the period 1996–2022. The 0.25°C isoline is dashed, while the continuous lines are at 1°C intervals. (d) Sill section showing the two ADCP sites (colored circles) with sound beams illustrated by colored cones. Black lines show two contours for average velocity toward 312°, see arrow in (b). (e) Average profiles of temperature (red), salinity (blue), and potential density (black) for the 400–800 m interval over the central sill based on 20 CTD profiles located in a small region around the ADCP sites. (f) Average velocity profiles for the 400–800 m interval at the two ADCP sites based on daily averaged profiles from 7,446 days at FB and 4,784 days at FC.

that the overflow component of the ISOW entrains ambient waters, roughly in a one-to-one ratio (Fogelqvist et al., 2003; Johns et al., 2021).

A one-to-one mixing ratio implies a doubling in transport, and Johns et al. (2021) found 5.3 Sv of ISOW to leave the Iceland Basin based on 4 years of moored observations within the "Overturning in the Subpolar North Atlantic Program" (OSNAP). Earlier estimates by Dickson and Brown (1994) and Sarafanov et al. (2012) emphasized that overflow with entrained ambient waters is the main contributor to the lower limb of the AMOC. OSNAP results have confirmed this (Lozier et al., 2019) and have enhanced the role of the ISOW (Johns et al., 2021; Petit et al., 2020). In terms of volume transport, the Iceland/Rockall basins account for almost half (48%) of the overturning east of Greenland, including the Arctic Mediterranean (i.e., north of the Greenland-Scotland Ridge, GSR) according to Koman et al. (2022). Petit et al. (2020) identified local buoyancy forcing south of the GSR as the primary mechanism. However, as emphasized by Koman et al. (2022), this does not represent the density

transformations, which are much more dramatic in the Arctic Mediterranean where the overflow waters are formed.

Since November 1995, temperature, salinity, and velocity of the FBC-overflow have been monitored by regular hydrographic surveys and moored instrumentation. Configuration of the monitoring system has been described by Hansen and Østerhus (2007) and Hansen et al. (2016), including average volume transports and seasonality.

Time series of FBC-overflow volume transport (Hansen et al., 2016) have shown a very stable transport. By contrast, the hydrographic properties of the FBC-overflow have been changing. This was indicated by Hansen et al. (2016), who found a warming of the bottom water from 2002 to 2014. Here, we report on the continued warming of the bottom water of the channel based on updated and reprocessed data (Hansen et al., 2023). We discuss concurrent changes in salinity and density of the FBC-overflow water and relate these changes to upstream sources for the FBC-overflow and to the Atlantic inflow. We propose that the observed warming implies a reduction in the density of the water fed into the deep limb of the AMOC.

2. Materials and Methods

Acoustic Doppler Current Profilers (ADCPs) have been deployed at two fixed sites over the FBC sill, FB and FC (Figures 1b and 1d). The deployments at FB began in November 1995, and those at FC started in July 2001. Data acquisition has been continuous except for annual servicing periods, typically lasting around 20 days, and occasional gaps due to mooring or instrument failure. The velocity profiles from the ADCPs have been quality controlled (see Hansen et al., 2016 for details). Since the deep part of the FBC is very narrow at the sill (Figure 1d), a value for the "kinematic volume transport" (i.e., based on velocity data) may be estimated from the ADCP profile at site FB alone (Hansen et al., 2016; Hansen & Østerhus, 2007).

Temperature at the ADCPs has been monitored, partly by the temperature sensor of the ADCP and partly by high-quality temperature loggers (SeaBird SBE37 or SBE39), which have been attached to the ADCP since 2001 at site FB and since 2015 at site FC. With the ADCPs at most 8 m above the bottom at both sites, the temperature at the instrument may be considered the bottom temperature within an accuracy of 0.001°C. The bottom temperature time series at sites FB and FC have been quality controlled and calibrated, as documented in a technical report (Hansen et al., 2023). The temperature observations from the high-quality temperature loggers have uncertainties of at most 0.01°C, but the ADCP temperature observations are more uncertain (Hansen et al., 2016). Comparison with adjacent conductivity-temperature-depth (CTD) profiles and attached high-quality temperature loggers have enabled re-calibrations that reduce the uncertainty of the ADCP temperature sensor to 0.02°C for annual averages (Hansen et al., 2023).

To facilitate annual average temperature estimates, two different methods have been employed to correct for the effect of the annual servicing periods and other occasional gaps on the bottom temperature at site FB (Hansen et al., 2023). The "Common period" temperature at FB, $T_{\mathrm{FB,Cp}}$, is the average of all daily values except for the period from day number 136 (mid-May) to day number 195 (mid-July) including most data gaps. The alternative, "Gap-filled", bottom temperature at FB, $T_{\mathrm{FB,Gf}}$, is corrected for gaps using an average "seasonal anomaly" (Hansen et al., 2023). At FC, bottom temperature is only calculated for the common period and is denoted T_{FC}.

To estimate hydrographic properties upstream of the FBC sill, we use SeaBird SBE911+ CTD data from regular (typically four times a year) occupations of 11 standard stations around the Faroes (Figure 1). These stations include two (V05 and V06) located just southeast of the sill, three stations on the S-section in the Faroe-Shetland Channel (FSC), and six stations on the N-section on the western boundary of the Norwegian Sea. The data have been quality controlled, and salinity calibrated against water samples. Their typical accuracy for overflow water is estimated at 0.001°C and 0.002 g kg^{-1} for salinity. Salinities are reported following TEOS-10 Absolute Salinity scale with δS_{A} set to zero (https://www.teos-10.org/), while temperatures are reported as Conservative Temperatures or in situ, when not specified.

3. Results

Average conditions are summarized in Figure 1 based on data updated to 2022. The bottom parts of the channel are dominated by the cold low-salinity overflow water (Figures 1c and 1e). The above-lying warmer and more saline water is a shallow and warm component of SPMW, which is traditionally termed "Atlantic inflow" (e.g., Hansen et al., 2016), since it is part of the Atlantic inflow to the Arctic Mediterranean, which is the main source

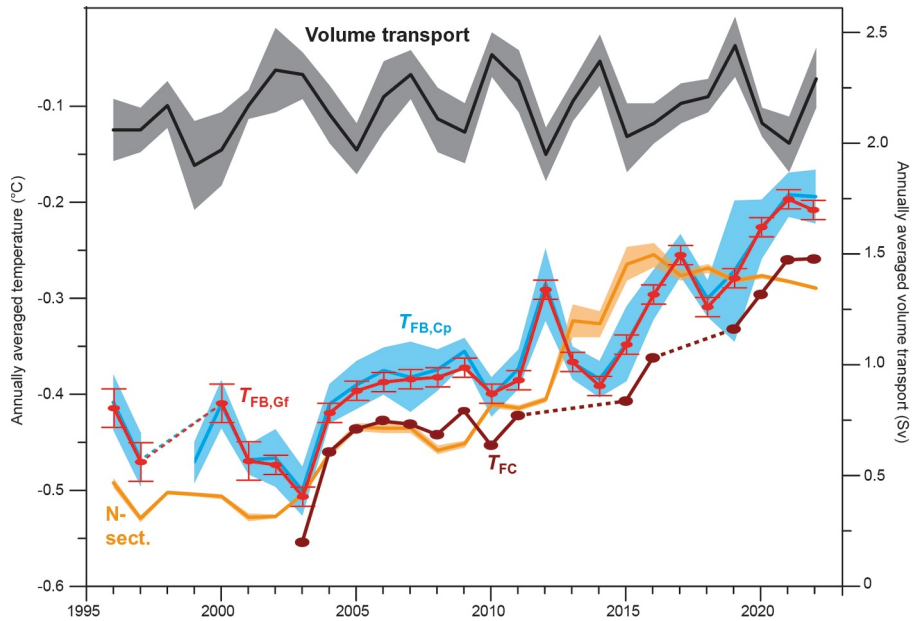

Figure 2. Temporal variations of FBC-overflow and upstream waters 1996–2022. The black curve at the top shows annually averaged kinematic volume transport of the FBC-overflow using the right-hand scale. All the other curves show annually averaged temperature using the left-hand scale. The bottom temperature at site FB is shown in cyan ($T_{FB,Cp}$), and red ($T_{FB,Gf}$), where error bars indicate the instrumental uncertainty of $T_{FB,Gf}$. The bottom temperature at site FC, T_{FC}, is shown in brown. Data gaps are indicated by dashed lines. The orange curve shows the average Conservative Temperature at the $\sigma_\Theta = 28.05$ kg m^{-3} isopycnal for water between N05 and N10 on the N-section. Semi-transparent areas with the same colors as the curves for volume transport (black), $T_{FB,Cp}$ (cyan), and N-section Conservative Temperature (orange) show average ± standard error where the standard errors for the two regular time series (volume transport and $T_{FB,Cp}$) have been corrected for serial correlation (von Storch, 1999).

water for the overflow (Hansen & Østerhus, 2000; Østerhus et al., 2019). The vertical velocity structure (Figures 1d and 1f) shows a relatively weak flow in the upper layers increasing to strong uni-directional flow in the overflow layer with average velocities exceeding 1 m s^{-1} in the core. Temporal variations of key parameters characterizing the FBC-overflow and upstream waters are illustrated in Figure 2.

3.1. Overflow Volume Transport

Annual values for the kinematic volume transport of the overflow water extend the time series presented in Hansen et al. (2016) by additional 8 years, maintaining the overall conclusion of stability with a long term mean of (2.2 ± 0.2) Sv. Over the whole period, the annual averages exhibit a slight positive trend, but it is not significantly different from zero (Figure 2).

3.2. The Temperature of the Bottom Water Over the FBC Sill

The two different estimates for the annual bottom temperature at FB are shown in Figure 2. They are almost identical and the difference is within the uncertainty estimate of 0.01°C, except for 2009 and 2022 where it is slightly higher. This implies that the annual average is not sensitive to the method used to account for the data gaps. The anomalously high temperature in 2012 raises suspicion. However, temperature data from FC, available only until late May, confirm the occurrence of concurrent warm pulses during spring 2012, which largely explain the anomaly.

Comparing data from 7 years with high-accuracy temperature loggers at both sites, Hansen et al. (2023) found the average difference between bottom temperature at FB and FC to be +0.07°C (T_{FB}–T_{FC}). Based on CTD data, most of this difference is not due to difference in bottom depth (30 m), but rather that the temperature at these depths decreases toward the Faroe Bank (Figures 1c and Hansen et al., 2023). On annual time scales, the bottom temperature at FB minus 0.07°C should therefore be a good estimator of the coldest overflow water crossing the Greenland-Scotland Ridge.

The time series of bottom temperature at FC has several gaps. The bottom water at FC is colder than at FB, but the temporal variation is similar at both sites. This confirms that the bottom water of the FBC has warmed throughout the monitoring period. From Figure 2, the warming started around 2004 and has continued since, although irregularly and with occasional reversing trends. For the six years with acceptable data before this start (1996–2003), the average value of $T_{FB,Gf}$ was −0.46°C. From this baseline, the bottom temperature increased to $T_{FB,Gf} = -0.21$°C for the last three years in our data set (2020–2022). The linear trend for the 2000–2022 period was (0.11 ± 0.02) °C per decade with a 95% confidence interval.

Most of the FBC-overflow is produced (leaves the surface) outside the Norwegian Sea (Brakstad et al., 2023; Huang et al., 2020), but it must pass through the Norwegian Sea, preferably over its western rim (Semper et al., 2020; Yang & Pratt, 2013) where it passes through the N-section (Figure 1). After crossing the section, it sometimes exhibits an eastward excursion before re-circulating back toward the Faroe-Shetland Channel (Chafik et al., 2020). According to Hátún et al. (2021), most of the overflow water passes between stations N05 and N10 (Figure 1a) and the orange curve in Figure 2 shows the Conservative Temperature for water between these two stations on the $\sigma_\Theta = 28.05$ kg m^{-3} isopycnal, which is similar to the potential density close to the bottom of the FBC (Figure 1e). The linear trend of this series was (0.12 ± 0.02) °C per decade with a 95% confidence interval, which is similar to the trend for $T_{FB,Gf}$. This result is not sensitive to the choice of stations on the N-section (Figure S1 in Supporting Information S1). We can therefore conclude that most of the warming at the bottom of the FBC sill since 2004 can be ascribed to warming of the upstream waters in the Norwegian Sea.

3.3. Vertical Extent of the Overflow Water Warming

The amount of CTD data over the FBC sill is not sufficient to estimate how far up into the overflow layer the observed bottom water warming extends. The data coverage is better at standard stations V05 and V06, a short distance upstream (Figure 1b), but there are still only a few CTD profiles a year and the temperature field is highly dynamic with strong short-term variations (Figure S2 in Supporting Information S1) that decrease the statistical significance of estimated trends. Instead, Figure 3a shows annually averaged temperatures at two other standard sections that should represent overflow water upstream of the sill. All the curves in Figure 3a indicate warming with similar trends that may collectively be expressed as (0.10 ± 0.03) °C per decade with 95% confidence limits. Upstream, waters at the same depths as the overflow layer over the FBC sill, thus, have warmed at the same rate as the FBC bottom water. However, ocean water tends to flow along constant potential density rather than constant depth. A more appropriate picture is presented in Figure 3b, which shows variations of the Conservative Temperature upstream on four isopycnals that cover most of the FBC-overflow layer (Figure 1e). Over the whole 1996–2022 period, all of the curves in Figure 3b exhibited statistically significant warming. For the $\sigma_\Theta = 28.05$ kg m^{-3} isopycnal on the N-section, the trend was (0.12 ± 0.02) °C per decade. However, after 2015, the warming appears to have stagnated at the denser levels and reversed for the lightest components.

3.4. Salinity Variations

Conductivity and pressure sensors associated with some of the high-accuracy temperature loggers (SBE37) allow salinity to be calculated, but the results are too unstable to provide a time series of overflow salinity. Instead, we use CTD data from standard stations upstream of the FBC sill. Given that salinity at fixed depth is highly variable with time, overflow salinity for each year at one of these stations is estimated as the average salinity at the same Conservative Temperature as the bottom water at ADCP site FB that year. With typical temperature and salinity values, the Conservative Temperature on the bottom at FB, Θ_{FB}, is equal to the in situ temperature minus 0.032°C, and we define $\Theta_{FB} = T_{FB,Gf}$–0.032°C. To estimate the bottom salinity at FBC each year, we therefore use the salinity at this Conservative Temperature upstream for that particular year.

The resulting time series of salinity at Conservative Temperature Θ_{FB} upstream of the FBC sill are shown in Figure 3c. Generally, the salinity increases as the overflow water proceeds from the S-section (blue) to station V06 (red) located approximately 20 km southeast of the sill. This increase may partly be explained by diapycnal mixing along the way from the S-section to the FBC sill area, which will tend to erode the salinity minimum around 0°C on the Θ–S curve (Figure S3 in Supporting Information S1, updated from Hansen et al., 2016). Alternatively, the salinity increase from the S-section to the V-section may be caused by entrainment of the more saline above-lying Atlantic inflow to the Arctic Mediterranean. Figure 3d shows three different time series of

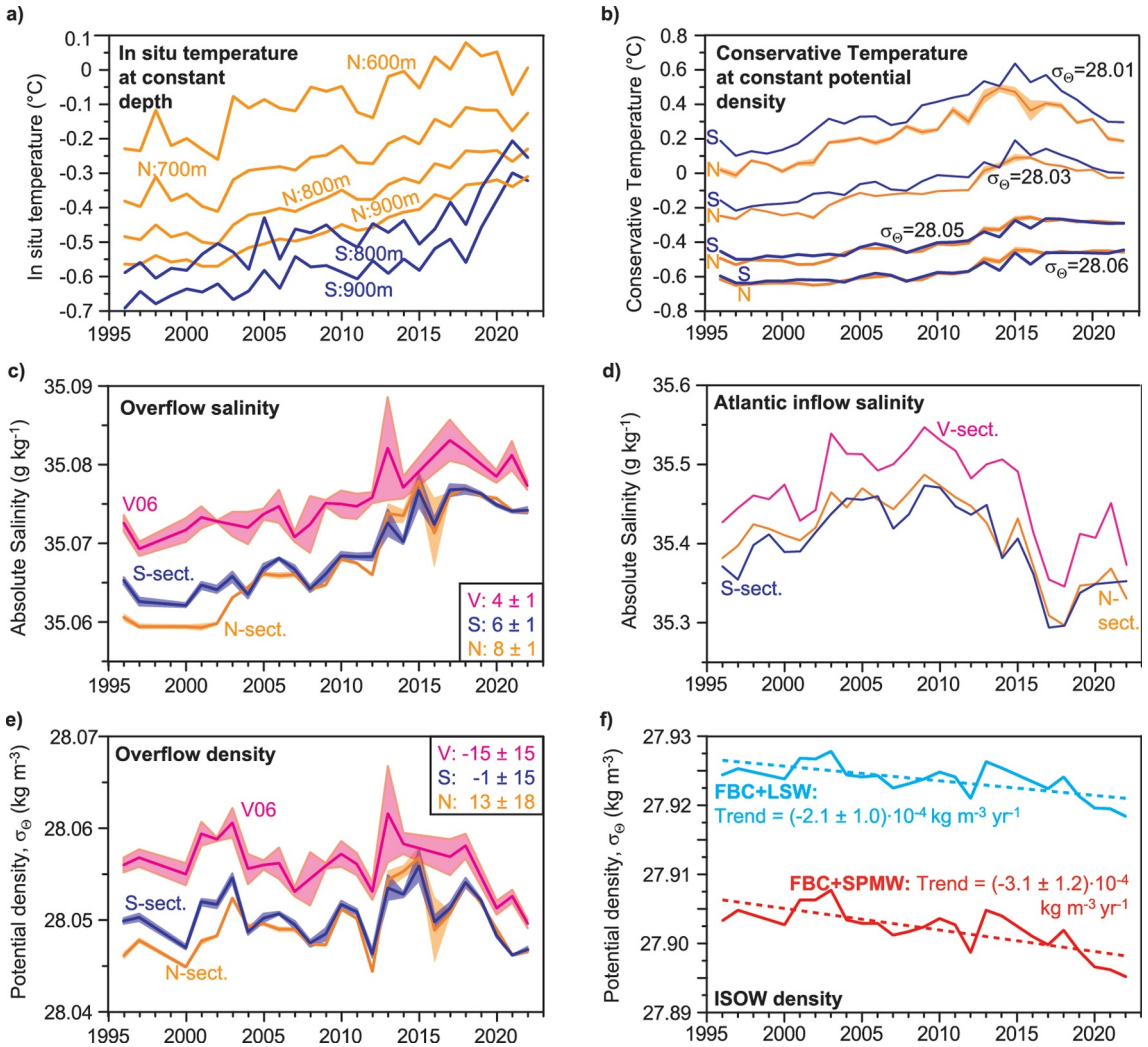

Figure 3. Temporal variations of temperature, salinity, and potential density at the locations indicated in Figure 1a. Results from standard sections have the same colors as the sections in Figure 1a. Semi-transparent areas around selected (to prevent visual overlap) curves show average ± one standard error. (a) In situ temperature at fixed depths on the N-section (orange) and on the S-section (blue). (b) Conservative Temperature on four isopycnal surfaces at the N-section (orange) and the S-section (blue). (c) Annually averaged salinity at V06 and on the S-section and N-section at the depths where the Conservative Temperatures are equal to the Conservative Temperature at the bottom of FB, Θ_{FB}, for the same year. The box in the lower right-hand corner shows linear trends with 95% confidence limits for the whole period in units of 10^{-3} g kg^{-1} (d) Annually averaged salinity of Atlantic inflow cores, defined as a 50 m deep layer with maximum average salinity along a section (V: magenta; N: orange) or shelf edge station (S: blue) (Larsen et al., 2012). (e) Annually averaged potential density, σ_Θ, on V06 and on the N-section, and the S-section at the depths where the Conservative Temperatures are equal to Θ_{FB} for the same year. The box in the upper right-hand corner shows linear trends with 95% confidence limits for the whole period in units of 10^{-4} kg m^{-3} (f) Annually averaged potential density, σ_Θ, of idealized ISOW generated as an equal mixture between bottom water from the FBC and either LSW or SPMW. The properties of LSW and SPMW were kept fixed, while the properties of the FBC bottom water each year had the Conservative Temperature Θ_{FB} and Absolute Salinity at Θ_{FB} on V06. The dashed lines are regression lines and the trends are listed with 95% confidence limits.

Atlantic inflow salinity. Their average values are different (Larsen et al., 2012), but they all have similar temporal variations with decreasing Atlantic inflow salinities after 2010 and especially after 2015 (Holliday et al., 2020).

Local entrainment of Atlantic inflow water into the overflow layer, therefore, cannot explain the temporal salinity increases in Figure 3c. Instead, this increase appears to be caused by salinity increases at the upstream sources. The overflow water is formed in the Arctic Mediterranean mainly from Atlantic inflow (Østerhus et al., 2019) by various regionally and temporally varying processes (e.g., Almeida et al., 2023; Eldevik et al., 2009). A lagged regression analysis indicates that variations of the overflow water properties may be seen as a lagged (by 8–18 years) and reduced (by a factor around five or more) response to changes in Atlantic inflow properties (Figure S4 in Supporting Information S1).

The motivation for using upstream salinity at the same Conservative Temperature as at the FBC sill the same year was based on the assumption of isopycnal flow. If this assumption holds, and salinity is conserved along the flow, then the choice of equal Conservative Temperatures implies equal potential density at the FBC sill and upstream. However, Figure 3c clearly shows that salinity is not conserved along the flow, particularly from the S-section to the V-section. Despite this, the three salinity curves in this figure have similar temporal trends. Additionally, station V06 is only 20 km upstream of the sill. Therefore, we argue that the temporal salinity increases upstream, especially at V06, imply a similar salinity increase at the FBC sill.

3.5. Implications for the Local Overturning and the AMOC

Based on this argument, the salinities from Figure 3c have been combined with the Conservative Temperature at site FB to calculate potential density each year (Figure 3e). Over the entire period 1996–2022, potential densities at the N-section and the S-section did not exhibit statistically significant trends. However, station V06 had a marginally significant negative trend, which was caused by a potential density decrease after 2015 (Figure 3e). During this period, the bottom temperature at ADCP site FB continued to rise (Figure 2) even though the Conservative Temperature remained almost constant at the two deepest isopycnals in Figure 3b. This might indicate that the bottom water over the FBC sill after 2015 has been drawn from slightly less dense, and therefore warmer, upstream waters due to deepening upstream isopycnals (Figure S5 in Supporting Information S1), conceivably caused by a lagged response to reduced Atlantic inflow salinity after 2010 (Figure 3d).

The evidence, however, is weak and we cannot claim that the density of the FBC-overflow decreased in the 1996–2022 period, which would directly impact the AMOC. Instead, the warming will have indirect impacts on the overturning in the Northeast Atlantic or the AMOC. As discussed in Sect. 1, the overflow water mixes roughly in a one-to-one ratio with ambient waters before leaving the Iceland Basin as ISOW. The ambient waters are mainly LSW and SPMW (Fogelqvist et al., 2003; Johns et al., 2021). The relative effect of temperature and salinity variations on density are different at high and low temperatures, which implies that when the overflow by entraining warmer water is raised to a higher temperature, its potential density becomes more sensitive to overflow temperature variations.

The effect of this is exemplified in Figure 3f, where we consider an idealized case with FBC bottom water mixing with equal amounts of either LSW or SPMW. The properties of LSW and SPMW are kept constant in time, equal to the values cited by Johns et al. (2021) (LSW: $\theta = 3.85$°C, $S_P = 34.92$ and SPMW: $\theta = 7$°C, $S_P = 35.2$) converted to Conservative Temperature and Absolute Salinity, whereas the properties of FBC bottom water vary every year according to the observations. While there is no significant trend in density for the undiluted overflow water within the FBC, the trend becomes highly significant after the overflow water has been raised to a higher temperature by entrainment. The recent large freshening seen in Atlantic inflow after 2015 (Holliday et al., 2020, Figure 3d) is likely yet to fully emerge in FBC salinity. Considering the estimated delay of 8–18 years, a freshening scenario may unfold in the very near future along with ongoing warming.

4. Conclusions

Annually averaged volume transport of FBC-overflow has remained relatively stable throughout the observational period from 1996 to 2022 (Figure 2). By contrast, the bottom temperature over the FBC sill has increased. The warming seems to have started around 2004. Over the observational period, the bottom temperature increased by around 0.25°C, equivalent to an average warming rate of 0.1°C per decade.

The warming over the bottom of the FBC is similar to and mainly caused by warming of the upstream waters at similar depths and isopycnals in the Norwegian Sea. CTD observations upstream also indicate that the warming extends far up into the overflow layer (Figures 3a and 3b).

Concurrent with the warming, the salinity of the FBC bottom water has also increased (Figure 3c) as a lagged and reduced response to the salinity variation of the Atlantic inflow (Figure 3d). This can also explain why the FBC bottom water salinity has remained relatively constant after 2015.

Due to the concurrent salinity increase, the warming has only caused a marginally significant trend of the potential density of the FBC bottom water, although there are indications of a decrease in the most recent years (Figure 3e). Despite this, the FBC-overflow, after entrainment of ambient water, likely contributed water of reduced density to

the overturning in the Iceland Basin and the AMOC. This is because of the warming of the overflow water and the effect of the non-linear dependence of density on temperature (Figure 3f).

Conflict of Interest

The authors declare no conflicts of interest relevant to this study.

Data Availability Statement

Time series of FBC overflow transport, FBC bottom temperature and Atlantic water properties are available as text files at http://envofar.fo/data/index.php?dir=Timeseries&sort=N&order=A. FBC current data and hydrographic data are available as text files at http://www.envofar.fo/index.php?page=climate.

Acknowledgments
We thank two anonymous referees for very constructive comments. We also thank colleagues at Havstovan and crew on R/V Magnus Heinason and R/V Jákup Sverri for their help with the Faroe Bank Channel moorings and data. The observations have been supported by the Danish Ministry of Climate, Energy and Utilities through its climate support program to the Arctic. This work has been supported by The National Centre for Climate Research (NCKF) hosted at the Danish Meteorological Institute, Denmark, by the Faroe-AMOC project (funded by Research Council Faroe Islands and NCKF), by the Blue Action project (EU Horizon, 2020 grant agreement nr. 727852), and by the ObsSea4Clim project (ObsSea4Clim "Ocean observations and indicators for climate and assessments" is funded by the European Union. Grant Agreement number: 101136548. 10.3030/101136548. Contribution nr. 3).

References

Almeida, L., Kolodziejczyk, N., & Lique, C. (2023). Large Scale Salinity Anomaly Has Triggered the Recent Decline of Winter Convection in the Greenland Sea. *Geophysical Research Letters*, *50*(21). https://doi.org/10.1029/2023GL104766

Beaird, N. L., Rhines, P. B., & Eriksen, C. C. (2013). Overflow waters at the Iceland-Faroe Ridge observed in multiyear seaglider surveys. *Journal of Physical Oceanography*, *43*(11), 2334–2351. https://doi.org/10.1175/JPO-D-13-029.1

Borenäs, K. M., & Lundberg, P. A. (1988). On the deep-water flow through the Faroe Bank Channel. *Journal of Geophysical Research*, *93*(C2), 1281–1292. https://doi.org/10.1029/JC093iC02p01281

Brakstad, A., Gebbie, G., Våge, K., Jeansson, E., & Ólafsdóttir, S. R. (2023). Formation and pathways of dense water in the Nordic Seas based on a regional inversion. *Progress in Oceanography*, *212*, 102981. https://doi.org/10.1016/j.pocean.2023.102981

Chafik, L., Hátún, H., Kjellsson, J., Larsen, K. M. H., Rossby, T., & Berx, B. (2020). Discovery of an unrecognized pathway carrying overflow waters toward the Faroe Bank Channel. *Nature Communications*, *11*(1), 3721. https://doi.org/10.1038/s41467-020-17426-8

Dickson, R., & Brown, J. (1994). The production of North Atlantic Deep Water: Sources, rates, and pathways. *Journal of Geophysical Research*, *99*(C6), 12319–12341. https://doi.org/10.1029/94JC00530

Eldevik, T., Nilsen, J. E., Iovino, D., Olsson, K. A., Sandø, A. B., & Drange, H. (2009). Observed sources and variability of Nordic seas overflow. *Nature Geoscience*, *2*(6), 406–410. https://doi.org/10.1038/ngeo518

Fogelqvist, E., Blindheim, J., Tanhua, T., Østerhus, S., Buch, E., & Rey, F. (2003). Greenland–Scotland overflow studied by hydro-chemical multivariate analysis. *Deep-Sea Research I*, *50*(1), 73–102. https://doi.org/10.1016/S0967-0637(02)00131-0

Geyer, F., Østerhus, S., Hansen, B., & Quadfasel, D. (2006). Observations of highly regular oscillations in the overflow plume downstream of the Faroe Bank Channel. *Journal of Geophysical Research*, *111*(C12), C12020. https://doi.org/10.1029/2006JC003693

Hansen, B., Larsen, K. M. H., Hátún, H., Mortensen, E., & Kristiansen, R. (2023). Quality control and calibration of Faroe Bank Channel bottom temperature. *Havstovan Technical Report Nr.: 23-03. Faroe Marine Research Institute*. Retrieved from https://pure.fo/ws/portalfiles/portal/42281216/TecRep2303.pdf

Hansen, B., Larsen, K. M. H., Hátún, H., & Østerhus, S. (2016). A stable Faroe Bank Channel overflow 1995-2015. *Ocean Science*, *12*(6), 1205–1220. https://doi.org/10.5194/os-12-1205-2016

Hansen, B., & Østerhus, S. (2000). North Atlantic-Nordic Seas exchanges. *Progress in Oceanography*, *45*(2), 109–208. https://doi.org/10.1016/S0079-6611(99)00052-X

Hansen, B., & Østerhus, S. (2007). Faroe Bank Channel overflow 1995–2005. *Progress in Oceanography*, *75*(4), 817–856. https://doi.org/10.1016/j.pocean.2007.09.004

Hátún, H., Chafik, L., & Larsen, K. M. H. (2021). The Norwegian Sea Gyre – a regulator of Iceland-Scotland Ridge exchanges. *Frontiers in Marine Science*, *8*, 694614. https://doi.org/10.3389/fmars.2021.694614

Hermann, F. (1959). Hydrographic observations in the Faroe Bank Channel and over the Faroe–Iceland ridge, june 1959. *Journal Du Conseil International Pour l'Exploration de La Mer*, *118*(5).

Holliday, N. P., Bersch, M., Berx, B., Chafik, L., Cunningham, S., Florindo-López, C., et al. (2020). Ocean circulation causes the largest freshening event for 120 years in eastern subpolar North Atlantic. *Nature Communications*, *11*(1), 585. https://doi.org/10.1038/s41467-020-14474-y

Huang, J., Pickart, R. S., Huang, R. X., Lin, P., Brakstad, E., & Xu, F. (2020). Sources and upstream pathways of the densest overflow water in the Nordic Seas. *Nature Communications*, *11*(1), 5389. https://doi.org/10.1038/s41467-020-19050-y

Johns, W. E., Devana, M., Houk, A., & Zou, S. (2021). Moored observations of the Iceland-Scotland Overflow plume along the eastern flank of the Reykjanes Ridge. *Journal of Geophysical Research: Oceans*, *126*(8). https://doi.org/10.1029/2021JC017524

Johnson, C., Sherwin, T., Cunningham, S., Dumont, E., Houpert, L., & Holliday, N. P. (2017). Transports and pathways of overflow water in the Rockall Trough. *Deep-Sea Research Part I Oceanographic Research Papers*, *122*, 48–59. https://doi.org/10.1016/j.dsr.2017.02.004

Koman, G., Johns, W. E., Houk, A., Houpert, L., & Li, F. (2022). Circulation and overturning in the eastern North Atlantic subpolar gyre. *Progress in Oceanography*, *208*, 102884. https://doi.org/10.1016/j.pocean.2022.102884

Larsen, K. M. H., Hátún, H., Hansen, B., & Kristiansen, R. (2012). Atlantic water in the Faroe area: Sources and variability. *ICES Journal of Marine Science*, *69*(5), 802–808. https://doi.org/10.1093/icesjms/fss028

Lozier, M. S., Li, F., Bacon, S., Bahr, F., Bower, A. S., Cunningham, S. A., et al. (2019). A sea change in our view of overturning in the subpolar North Atlantic. *Science*, *363*(6426), 516–521. https://doi.org/10.1126/science.aau6592

Mauritzen, C., Price, J., Sanford, T., & Torres, D. (2005). Circulation and mixing in the Faroese Channels. *Deep-Sea Research I*, *52*(6), 883–913. https://doi.org/10.1016/j.dsr.2004.11.018

Østerhus, S., Sherwin, T., Quadfasel, D., & Hansen, B. (2008). The overflow transport east of Iceland. In R. R. Dickson, P. Rhines, & J. Meincke (Eds.), *Arctic-subarctic ocean fluxes* (pp. 427–441). Springer. https://doi.org/10.1007/978-1-4020-6774-7_19

Østerhus, S., Woodgate, R., Valdimarsson, H., Turrell, B., De Steur, L., Quadfasel, D., et al. (2019). Arctic Mediterranean exchanges: A consistent volume budget and trends in transports from two decades of observations. *Ocean Science*, *15*(2), 379–399. https://doi.org/10.5194/OS-15-379-2019

Petit, T., Lozier, M. S., Josey, S. A., & Cunningham, S. (2020). Atlantic Deep Water formation occurs primarily in the Iceland Basin and Irminger Sea by local buoyancy forcing. *Geophysical Research Letters*, *47*(22). https://doi.org/10.1029/2020GL091028

Sarafanov, A., Falina, A., Mercier, H., Sokov, A., Lherminier, P., Gourcuff, C., et al. (2012). Mean full-depth summer circulation and transports at the northern periphery of the Atlantic Ocean in the 2000s. *Journal of Geophysical Research*, *117*(C1), C01014. https://doi.org/10.1029/2011JC007572

Semper, S., Pickart, R. S., Våge, K., Larsen, K. M. H., Hátún, H., & Hansen, B. (2020). The Iceland-Faroe Slope Jet: A conduit for dense water toward the Faroe Bank Channel overflow. *Nature Communications*, *11*(1), 5390. https://doi.org/10.1038/s41467-020-19049-5

Ullgren, J. E., Darelius, E., & Fer, I. (2016). Volume transport and mixing of the Faroe Bank Channel overflow from one year of moored measurements. *Ocean Science*, *12*(2), 451–470. https://doi.org/10.5194/OS-12-451-2016

von Storch, H. (1999). Misuses of statistical analysis in Climate Research. In H. von Storch & A. Navarra (Eds.), Analysis of climate *variability*. Springer. https://doi.org/10.1007/978-3-662-03744-7_2

Yang, J., & Pratt, L. J. (2013). On the effective capacity of the dense-water reservoir for the nordic seas overflow: Some effects of topography and wind stress. *Progress in Oceanography*, *43*(2), 418–431. https://doi.org/10.1175/JPO-D-12-087.1